Compilation of $\pi^- p$ Data at 4 GeV/c: Backward Resonance Production and $\pi\pi$ Scattering*†

P. B. JOHNSON, J. A. POIRIER, N. N. BISWAS, N. M. CASON, T. H. GROVES, V. P. KENNEY, J. T. MCGAHAN, AND W. D. SHEPHARD
Department of Physics, University of Notre Dame, Notre Dame, Indiana 46556

AND

L. J. GUTAY, J. H. CAMPBELL, R. L. EISNER, F. J. LOEFFLER, R. E. PETERS, R. J. SAHNI, AND W. L. YEN
Department of Physics, Purdue University, Lafayette, Indiana 47907

AND

I. DERADO AND Z. G. T. GUIRAGOSSIÁN
Stanford Linear Accelerator Center, Stanford University, Stanford, California 94305

(Received 26 July 1968)

In $\pi^- p$ single-pion-production reactions near 4 GeV/c, we observe several interesting features. Backward ρ^0 production is seen to occur with $d\sigma/du = 63 \pm 21$ μb/(GeV/c)^2 at 180°. Backward ρ^- production is less prominent. We see evidence for production at small u of N^{*0} ($p\pi^-$ near 1700 MeV) and Δ^- ($n\pi^-$ at 1236 MeV), and possible evidence for other $n\pi^-$ structure at about 1800 MeV. The density-matrix elements for peripheral ρ^0 production are presented in the Jackson and in the helicity frame. The $\pi^+\pi^-$ elastic cross section is obtained by extrapolation of the data to the mass shell. The S-wave $\pi\pi$ phase shifts are calculated by two methods and compared with previous results. We find evidence in the dipion decay angular distribution for the $\pi^+\pi^-$ decay mode of the $S^*(1070)$.

I. INTRODUCTION

THE results presented here are obtained from a study of single-pion production in $\pi^- p$ interactions at incident momenta of 3.65, 3.90, 4.0, and 4.16 GeV/c.[1] The weighted average incident momentum is 4.0 GeV/c. We have 7916 events of the type

$$\pi^- p \rightarrow \pi^+\pi^- n \tag{1}$$

and 4978 events of the type

$$\pi^- p \rightarrow \pi^0\pi^- p. \tag{2}$$

The weighted total cross sections are 3.12 ± 0.05 mb for reaction (1) and 2.10 ± 0.04 mb for reaction (2). Reactions (1) and (2) at these energies are dominated by peripheral ρ^0, f^0, and ρ^- production. Isobar production has been observed to occur about 8% of the time in reaction (1) and 20% in reaction (2).[1]

We examine the following three important characteristics of the above reactions: backward resonance production, ρ production and decay, and $\pi\pi$ scattering. In Sec. II, we discuss u-channel production of resonances. In Sec. III, ρ and f^0 production and decay are discussed. The ρ-decay density-matrix elements are given in both the Jackson frame, in which the quantization axis is the incident π^- direction, and the helicity frame, in which the quantization axis is the ρ line of flight. In Sec. IV we analyze the peripherally produced dipion events in terms of $\pi\pi$ scattering. In discussing angular distributions we will use the convention that θ_{ab}^* refers to the angle between incoming particle a and outgoing b in the over-all center-of-mass (c.m.) system and θ_{ab} refers to the angle between incoming particle a and outgoing particle b in the appropriate two-particle rest system.

II. u-CHANNEL RESONANCE PRODUCTION

Figure 1 shows the $\pi^+\pi^-$ effective-mass distributions for events in which the dipion system is produced in the

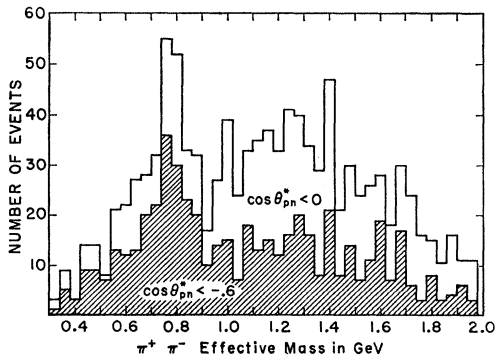

FIG. 1. The $\pi^+\pi^-$ effective mass spectrum for events with $\cos\theta_{pn}^* < 0.0$ (full histogram), $\cos\theta_{pn}^* < -0.6$ (shaded histogram).

* Work supported in part by the Atomic Energy Commission and the National Science Foundation.

† Notre Dame-Purdue-SLAC Collaboration.

[1] 3.65 GeV/c—Y. Y. Lee, B. P. Roe, D. Sinclair, and J. C. Vander Velde, Phys. Rev. Letters **12**, 342 (1964); R. W. Birge, R. R. Ely, T. S. Schuman, Z. G. T. Guiragossián, and M. Whitehead, in *Proceedings of the Twelfth International Conference on High Energy Physics, Dubna, 1964* (Atomizdat, Moscow, 1965), p. 153; 4.0 GeV/c—Aachen-Birmingham-Bonn-Hamburg-London (I.C.)-Munich Collaboration, Nuovo Cimento **31**, 729 (1964); 4.0 GeV/c—I. Derado, V. P. Kenney, J. A. Poirier, and W. D. Shephard, Phys. Rev. Letters **14**, 872 (1965); 4.16 GeV/c—R. L. Eisner, P. B. Johnson, P. R. Klein, R. E. Peters, R. J. Sahni, W. L. Yen, and G. W. Tautfest, Phys. Rev. **164**, 1699 (1967). We have included in our analysis only those events from the above experiments which are unambiguous, i.e., the positive track is identifiable by ionization or only one satisfactory fit is obtained.

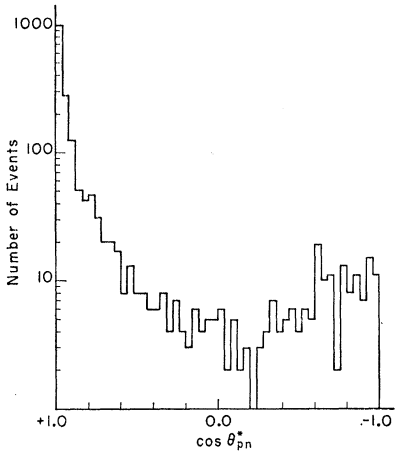

FIG. 2. Number of events in the ρ^0 band (0.70 → 0.85 GeV) as a function of $\cos\theta_{pn}^*$, the cosine of the c.m. scattering angle.

backward hemisphere, i.e., $\cos\theta_{pn}^*<0$. The shaded histogram is the subsample with $\cos\theta_{pn}^*<-0.6$. We see a clear ρ^0 signal above background for both selection criteria; in contrast, we see no significant evidence for f^0 or any other structure for $\cos\theta_{pn}^*<-0.6$. Using a smooth background for this mass spectrum and correcting for losses in the tails of a Breit-Wigner curve for the ρ^0 intensity, we estimate the ρ^0 production cross section to be 87 ± 15 μb for backward production ($\cos\theta_{pn}^*<0$).

From the mass spectra shown in Fig. 1, we estimate that about 50% of the events in the ρ^0 region are background; within statistics, this fraction is independent of $\cos\theta_{pn}^*$ in the interval $-0.3\leq\cos\theta_{pn}^*<-1.0$. Thus, we have calculated the differential cross section for the backward region using the number of events in the ρ^0 region and the total cross section of 87 μb as mentioned before. Figure 2 shows the c.m. ρ^0 angular distribution. The differential cross section seems to rise in the backward direction although the hypothesis of constant cross section is consistent with the data (at the 20% confidence level). We estimate the ρ^0 differential cross section near 180° to be 63 ± 21 μb/(GeV/c).[2]

The production mechanism for ρ^0 in the backward direction is a topic of some interest. In Fig. 3 we have plotted the dipion-decay angular distribution for three different production regions. In the forward region, $\cos\theta_{pn}^*>0.6$, the distribution in $\theta_{\pi^-\pi^-}$ shows the $\cos^2\theta_{\pi^-\pi^-}$ contribution from one-pion exchange and a strong forward asymmetry. In contrast, the decay distributions for $\cos\theta_{pn}^*<0.6$ show no asymmetry and are consistent with isotropy. If baryon exchange contributes to backward production, the ρ is produced at the proton vertex; in this case the quantization axis becomes the incident proton direction. The resulting distributions in $\cos\theta_{p\pi^-}$ and $\phi_{p\pi^-}$ for $\cos\theta_{pn}^*<-0.6$ are shown in Fig. 4. Both of these distributions are consistent with isotropy. To examine effects on these distributions due to background present under the ρ peak, we have looked at the corresponding distributions for events on both sides of the ρ. The distributions of Figs. 4(a) and 4(b) are not altered after subtraction of these background distributions. These results are consistent with predictions for exchange of an unpolarized nucleon.

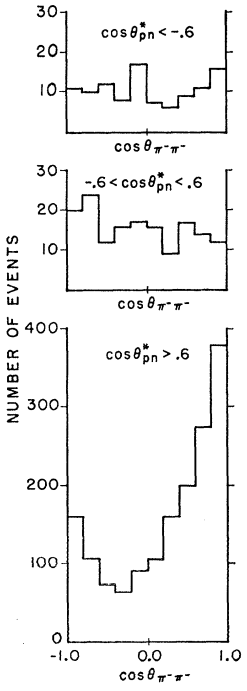

FIG. 3. The $\pi^+\pi^-$ decay angular distribution in the ρ band (0.70 → 0.85 GeV) for three intervals in the c.m. angle θ_{pn}^*.

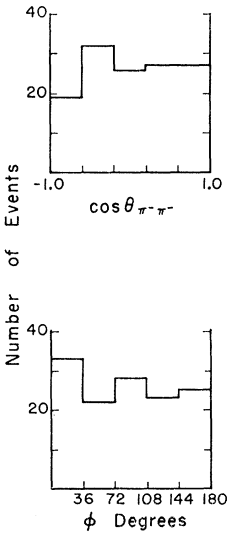

FIG. 4. Decay angular distributions for events in the ρ^0 band (0.70 → 0.85 GeV) with $\cos\theta_{pn}^*<-0.6$.

[2] P. Bareyre, C. Bricman, and G. Villet, Phys. Rev. **165**, 1730 (1968); C. H. Johnson, P. D. Grannis, M. J. Hansroul, O. Chamberlain, G. Shapiro, and H. M. Steiner, University of California Radiation Laboratory Report No. UCRL-17683, 1967 (unpublished); A. Donnachie, R. G. Kirsopp, and C. Lovelace, CERN Report No. TH838, 1967 (unpublished).

In reactions (1) and (2), if backward ρ production is interpreted in terms of a Reggeized baryon-exchange model, the N_α, N_γ, and Δ trajectories can all contribute to ρ^0 production whereas only Δ exchange can contribute to ρ^- production. In Fig. 5(a) we show the $\pi^0\pi^-$ effective-mass distribution for events with $\cos\theta_{pp}^* < -0.6$. For comparison, Fig. 5(b) shows a strong ρ^- signal in the $\pi^0\pi^-$ distribution for all events. We estimate the ρ^- signal in Fig. 5(a) to be 18 ± 5 events; this corresponds to about $\frac{1}{4}$ the ρ^0 signal seen in the shaded distribution of Fig. 1. This suggests that Δ exchange is weaker than nucleon exchange for backward ρ production. When we look at the production angular distribution for the $\pi^-\pi^0$ system in Fig. 6, we observe a sharp increase in the differential cross section at the last bin ($\cos\theta_{pp}^* < -0.96$), which suggests Δ^{++} exchange. However, we are not able to associate this peaking with resonance production in the dipion system.

Figure 7(a) shows the neutron π^- effective mass spectrum for events which have $\cos\theta_{\pi^-\pi^+} < -0.6$ and which lie outside the ρ^0 band (0.70 to 0.85 GeV). We observe a strong Δ^-_{1236} signal and possible evidence for other structure at 1.80 and 1.96 GeV. Both of these latter enhancements are 2 to 3 standard-deviation effects. The steeply rising background in Fig. 7(a) comes from events in which the dipion system is peripherally produced. We can effectively suppress this background by making cuts in $\cos\theta_{pn}^*$; the shaded events in Fig. 7(a) are removed when $\cos\theta_{pn}^* < 0.9$. (The two enhancements remain significant even when we make the more stringent cut $\cos\theta_{pn}^* < 0.8$.) In 7(b) the corresponding spectrum is shown for the middle region $-0.6 < \cos\theta_{\pi^-\pi^+}^*$

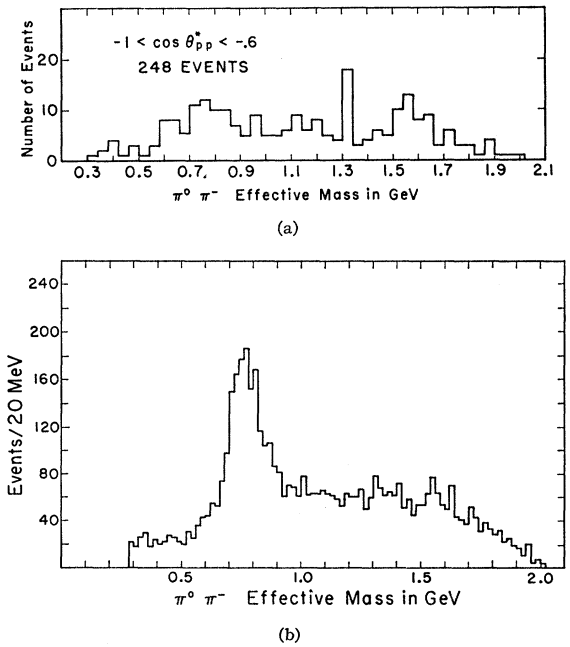

FIG. 5. The $\pi^0\pi^-$ effective mass spectrum. (a) Events with $\cos\theta_{pp}^* < -0.6$. (b) All events.

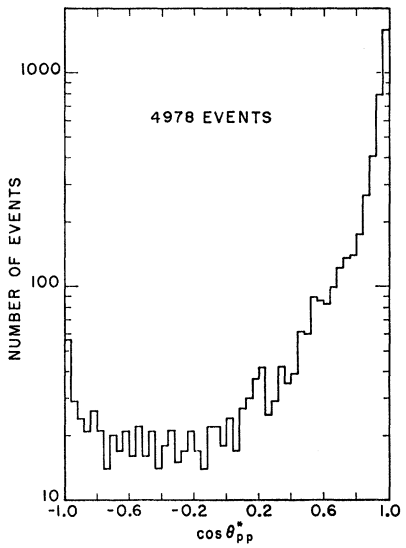

FIG. 6. Differential cross section for $\pi^-\rho \rightarrow \pi^0\pi^-\rho$.

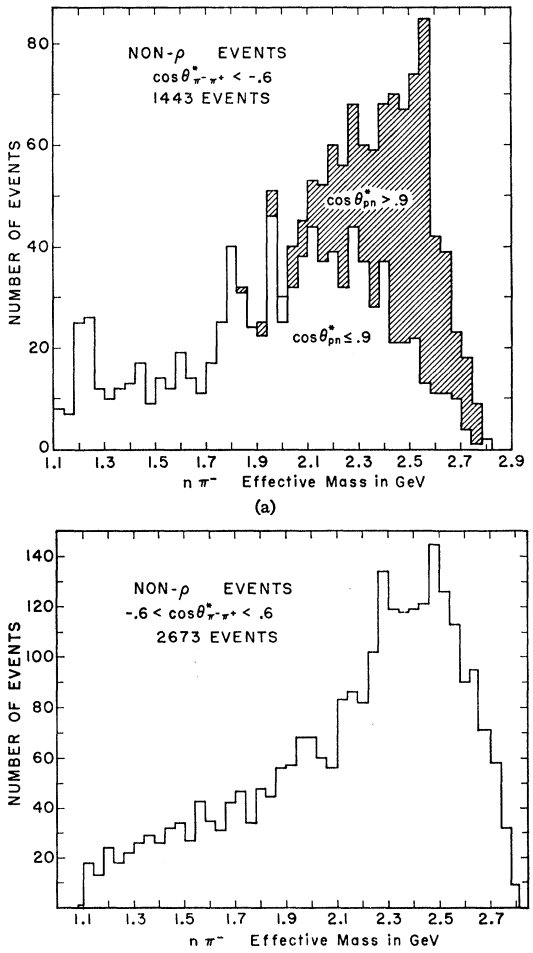

FIG. 7. The $n\pi^-$ effective mass spectrum. All events for which the $\pi^+\pi^-$ effective mass is in the ρ band (0.70 → 0.85 GeV) have been excluded. (a) $\cos\theta_{\pi^-\pi^+}^* < -0.6$. The shaded events are those for which $\cos\theta_{pn}^* > 0.9$. (b) $-0.6 < \cos\theta_{\pi^-\pi^+}^* < 0.0$.

TABLE I. Maximum likelihood fits to the mass spectrum in Fig. 11. Fit function No. 1 is Eqs. (3) and (5). Fit functions Nos. 2–5 are Eqs. (4) and (5) (mass-squared fit). $F_1=(M/M_0)(Q_0/Q)$, where $Q^2=(\frac{1}{2}M)^2-m^2$, $Q_0^2=(\frac{1}{2}M_0)^2-m^2$. $\Gamma_1=\Gamma_0(Q/Q_0)^3D_0/D$, where $D=1.0+(Q/0.777)^2$ and $\Gamma_2=\Gamma_0(Q/Q_0)^3(M_0/M)$. Of the fits tried, fit No. 4 is the best fit in terms of $\ln(LF)$.

Fit function	$\ln(LF)$	Γ	F	A_1	M_1	Γ_1	ρ^0/Tot	A_2	M_2	Γ_2
1 (M)	−3.26	const	1.0	0.467	0.776	0.152	0.368	0.168	1.266	0.195
2 (M^2)	−17.06	const	1.0	0.522	0.780	0.142	0.340	0.586	1.266	0.216
3 (M^2)	−9.08	const	F_1	0.543	0.776	0.148	0.382	0.748	1.264	0.210
4 (M^2)	0.0	Γ_1	F_1	0.555±0.021	0.775±0.002	0.154±0.006	0.404±0.015	0.618±0.04	1.268±0.006	0.176±0.013
5 (M^2)	−2.03	Γ_2	F_1	0.548	0.776	0.152	0.394	0.673	1.266	0.191
average				0.527±0.033	0.777±0.002	0.150±0.004	0.377±0.022	0.656±0.04	1.266±0.006	0.197±0.013

<0.6. We note that the Δ^-_{1236}, the 1.80-GeV, and the 1.96-GeV enhancements are not present. We suggest that these enhancements are not due to any known backward effects and that they may be interpreted as isospin-$\frac{3}{2}$ isobars. Studies of the decay distributions are not statistically significant. Phase-shift analyses[2] have reported evidence for several new $I=\frac{3}{2}$ isobars not previously seen, including a P_{31} resonance at 1.934 and a D_{35} at 1.954 GeV. However, there is no reported structure at 1.80 GeV in the phase-shift analyses.

The other system for which nucleon exchange is allowed is the $p\pi^-$ combination. The $p\pi^-$ effective mass is plotted in Fig. 8 for $\cos\theta_{n^-n^0}<-0.6$. We observe a signal near 1.68 GeV where several $I=\frac{1}{2}$ isobars have been reported. There is no evidence for a 1.80- or 1.96-GeV enhancement, but this is not unexpected, since the Clebsch-Gordan coefficient is unfavorable for producing $I=\frac{3}{2}$ systems. In contrast to the above, the backward $n\pi^+$ and $p\pi^0$ systems require doubly charged isobar exchange in the u channel. The mass spectra for these systems, Figs. 9 and 10, show no interesting structure. Thus we conclude that within the limits of our statistics isobar production, like boson production, proceeds predominantly via nucleon exchange.

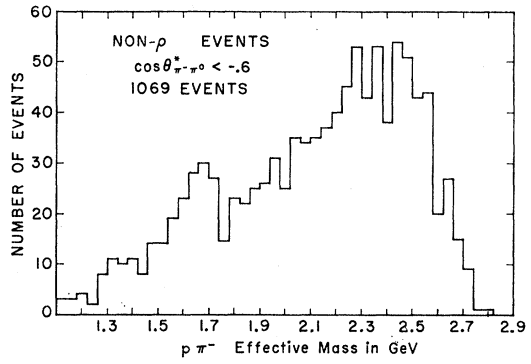

FIG. 8. The $p\pi^-$ effective-mass spectrum for events with $\cos\theta_{\pi^-\pi^0}^*<-0.6$. All events for which the $\pi^0\pi^-$ effective mass is in the ρ band (0.70 → 0.85 GeV) have been excluded.

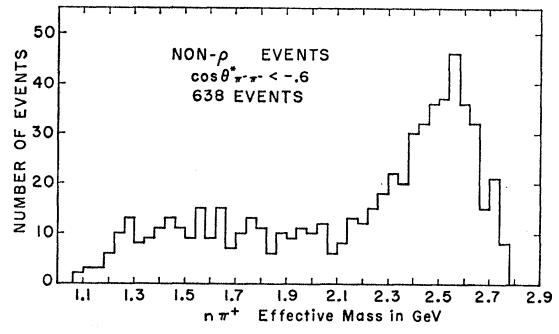

FIG. 9. The $n\pi^+$ effective-mass spectrum for events with $\cos\theta_{n\pi^-}^*<-0.6$. All events for which the $\pi^+\pi^-$ effective mass is in the ρ band (0.70 → 0.85 GeV) have been excluded.

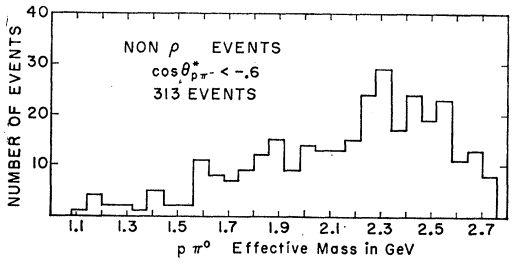

FIG. 10. The $p\pi^0$ effective-mass spectrum for events with $\cos\theta_{p\pi^-}^*<-0.6$. All events for which the $\pi^0\pi^-$ effective mass is in the ρ band (0.70 → 0.85 GeV) have been excluded.

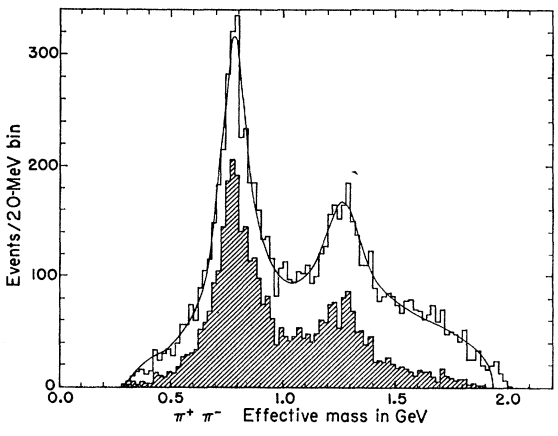

FIG. 11. The $\pi^+\pi^-$ effective mass spectrum. The shaded events are those with $\cos\theta_{p\pi}^*\geq 0.94$. The fitted curve is obtained assuming constant width resonances and phase space.

III. $\pi\pi$ RESONANCES

Figure 11 shows the invariant-mass spectrum for reaction (1) for all the data; the shaded histogram shows events with $\cos\theta_{pn}^* \geq 0.94$, a cut which, for a dipion mass of 0.775 GeV, corresponds to $|t| < 0.2(\text{GeV}/c)^2$. The ρ^0 and f^0 resonances are prominent: about 40% of the events correspond to ρ^0 production and 14% to f^0 production. The solid curve in Fig. 11 is a fit to the data, assuming two constant-width Breit-Wigner shapes for the ρ^0 and the f^0 plus phase space for the background. More details of the fitting procedure and the values of the fitted parameters are discussed below.

Figures 12(a) and 12(b) show two Dalitz plots for reaction (1); two plots are shown since the third two-particle effective mass for a point is dependent on the incident momentum. Figure 13 is a Chew-Low scatter plot of $M(\pi^+\pi^-)$ versus $(-t/\mu^2)^{\frac{1}{2}}$ for reaction (1), where μ is the pion mass. There is a strong concentration of events near the minimum allowable momentum transfer. There is also some increase in the density of events near the maximum allowable momentum transfer; these events have been discussed in Sec. II.

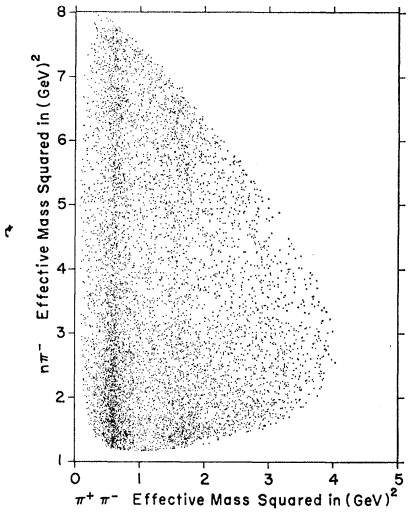

FIG. 12. Dalitz plots for the reaction $\pi^- p \to \pi^0\pi^- p$. (a) $n\pi^-$ effective mass squared versus $\pi^+\pi^-$ effective mass squared. (b) $n\pi^-$ effective mass squared versus $n\pi^+$ effective mass squared.

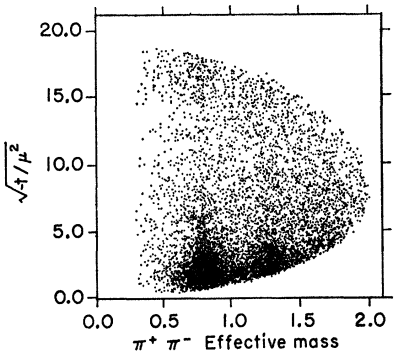

FIG. 13. Scatter plot of $(-t/\mu^2)^{1/2}$ versus the $\pi^+\pi^-$ effective mass.

Figure 14 is a scatter plot of $\cos\theta_{\pi^-\pi^-}$ versus the $\pi^+\pi^-$ invariant mass. The strong forward-backward asymmetry for the ρ^0 region is apparent; the distribution is rather symmetrical in the f^0 region but becomes quite sharply peaked near $\cos\theta = +1.0$ for masses above the f^0. The cluster of events near $\cos\theta_{\pi^-\pi^-} = \pm 1$ at 1.0 GeV will be discussed in Sec. IV.

Table I summarizes various maximum likelihood fits to the mass spectrum in Fig. 11. We have used various forms of the expected Breit-Wigner shapes[3]:

$$\text{BW} = A\tfrac{1}{2}\Gamma F/[(M-M_0)^2+(\tfrac{1}{2}\Gamma)^2] \quad (3)$$

and

$$\text{BW} = A\Gamma F/[(M^2-M_0^2)^2+M^2\Gamma^2], \quad (4)$$

where A is the intensity, F is a function defined in Table I, M_0 is the resonance mass, and Γ is the full width at

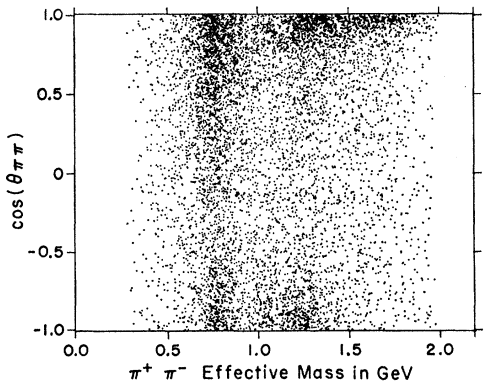

FIG. 14. Scatter plot of $\cos\theta_{\pi^-\pi^-}$ versus the $\pi^+\pi^-$ effective mass.

[3] J. D. Jackson, Nuovo Cimento 43, 1644 (1964).

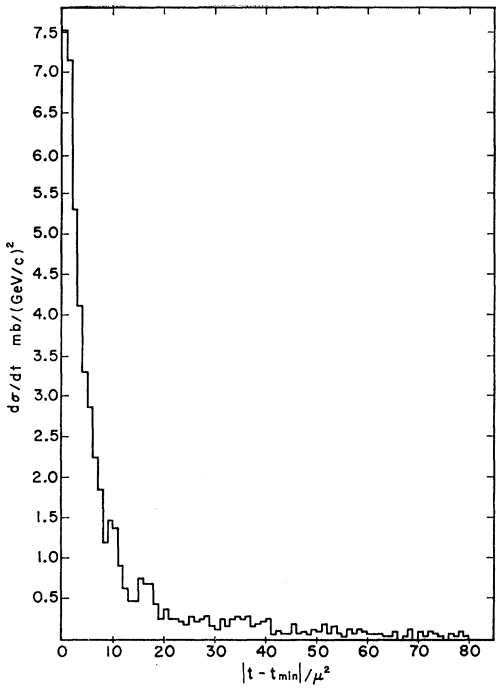

FIG. 15. $d\sigma/dt$ for ρ^0 production normalized to a total ρ^0 cross section of 1.15 mb.

half-maximum for the resonance. The over-all fit function is

$$dN/dM = (\mathrm{PS})[1.0 + (\mathrm{BW})_\rho + \mathrm{BW})f], \qquad (5)$$

where PS is three-body phase space. Fit errors are shown for fit number 4; the other fits have comparable errors. Note that the fraction of ρ^0 varies from 0.340 to 0.404, depending on the function used.

If one takes the average (ρ^0/total=0.377), the total ρ production cross section at GeV/c falls in the range 1.06 to 1.26 mb based on the fits in Table I. Figure 15 shows the t distribution for ρ^0 production scaled so that the total cross section is 1.15 mb; the shape of the distribution is obtained from all events with effective dipion mass in the interval 0.70–0.85 GeV. From the fits, we estimate that this mass interval contains 18% non-ρ background.

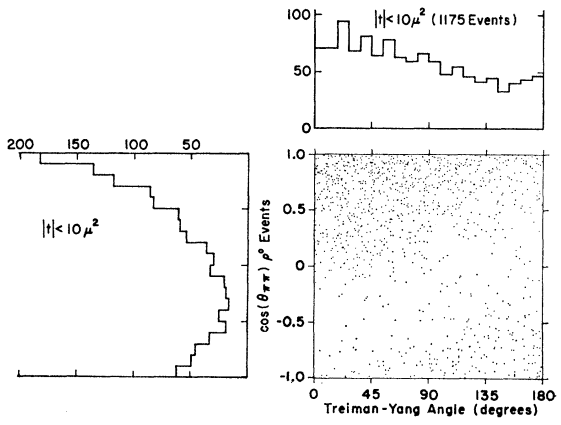

FIG. 16. Cos$\theta_{\pi^-\pi^-}$ versus ϕ for $\pi^+\pi^-$ effective mass in the ρ^0 band (0.75 → 0.85 GeV) and $|t|<0.2$ (GeV/c)².

In Fig. 16 we show a scatter plot of cos$\theta_{\pi^-\pi^-}$ versus the Treiman-Yang angle together with the projections on the axes. The nonuniform distribution of events on this scatter plot has been fitted with a function parametrized by density-matrix elements ρ_{mn} which includes possible S- and P-wave interference effects.[4] The t dependence of these matrix elements is presented in Figs. 17 and 18.

Interest in the vector-dominance model has focused attention on the density-matrix elements in the dipion helicity frame. We have evaluated the density-matrix elements in the helicity frame as a function of t; the results of the fits are shown in Figs. 19 and 20.

IV. ππ SCATTERING

It has been observed previously[1] that ρ^0 production and decay can be fairly well explained for small values of $|t|$ by models based on one-pion exchange, e.g., the absorption model[5] (cf. Figs. 17 and 18). We have also seen in Fig. 13 that reaction (1) is peripheral not only in the ρ^0 and f^0 resonance bands but across the entire

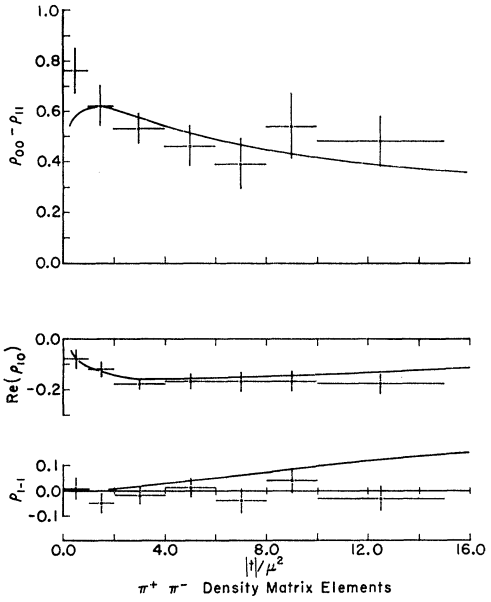

FIG. 17. The t dependence of the density-matrix elements for events in the ρ^0 band (0.70 → 0.85 GeV). The curves are taken from an absorption-model calculation which includes S- and P-wave interference (Ref. 4).

[4] P. B. Johnson, L. J. Gutay, R. L. Eisner, P. R. Klein, R. E. Peters, R. J. Sahni, W. L. Yen, and G. W. Tautfest, Phys. Rev. **163**, 1497 (1967).

[5] K. Gottfried and J. D. Jackson Nuovo Cimento **34**, 735 (1964); L. Durand, III, and Y. T. Chiu, Phys. Rev. **139**, B646 (1965).

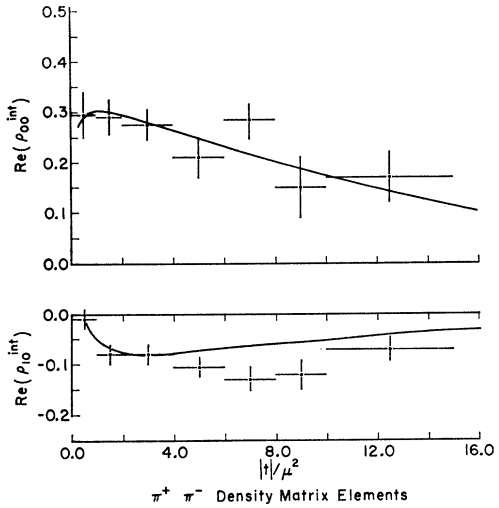

FIG. 18. The t dependence of the S- and P-wave interference density-matrix elements for events in the ρ^0 band ($0.70 \rightarrow 0.85$ GeV). The curves are taken from Ref. 4.

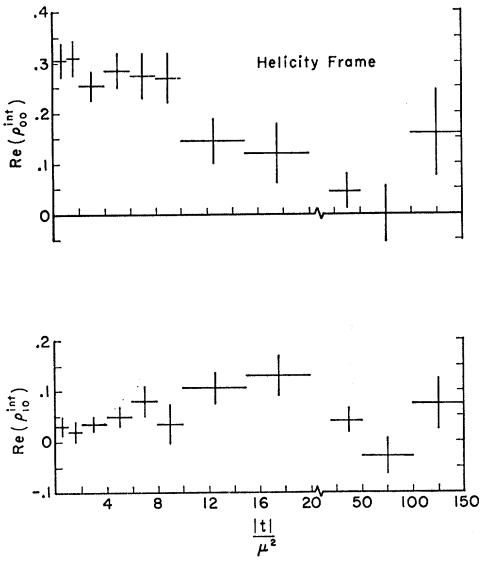

FIG. 20. The t dependence of the S- and P-wave interference density-matrix elements for events in the ρ^0 band ($0.70 \rightarrow 0.85$ GeV).

dipion mass spectrum. Similar observations have been made in other experiments.[6] Thus there is considerable evidence suggesting that for small $|t|$ the dipion-decay angular distributions from reaction (1) contain information related to $\pi\pi$ elastic scattering. The question of obtaining the S-wave $\pi\pi$ phase shifts from data on reactions (1) and (2) is a topic of current concern.

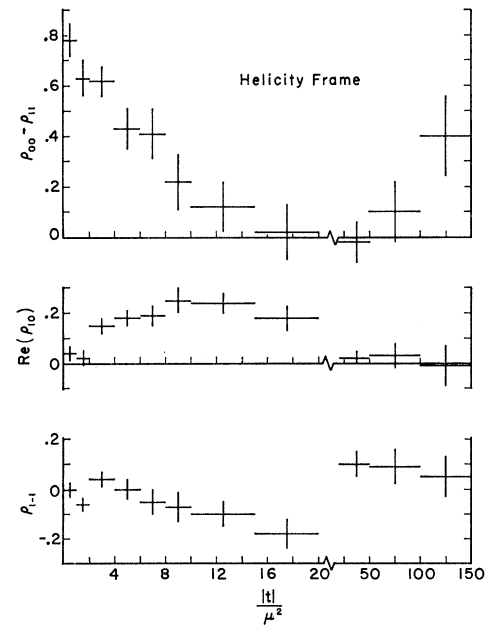

FIG. 19. The t dependence of the density-matrix elements in the ρ helicity frame for events in the ρ^0 band ($0.70 \rightarrow 0.85$ GeV).

Gutay *et al.*[7] observed that the t dependence of the dipion-decay distribution was fitted rather well by an absorption-model calculation which included S-wave amplitudes. Applying this model to data from reaction (1) at 2.7 GeV/c, they obtained two sets of $I=0$ S-wave phase shifts. The same model was applied to slightly more than half the data in the present collaboration, and the results were in quite good agreement with those obtained previously.[4] It should be pointed out that in the calculation of the $\pi\pi$ S-wave phase shifts one encounters two types of ambiguities. An unavoidable ambiguity results from the invariance of the scattering amplitude ($\propto e^{i\delta}\sin\delta$) under the transformation $\delta \rightarrow \delta \pm n\pi$. The second ambiguity, in analyses based on S-

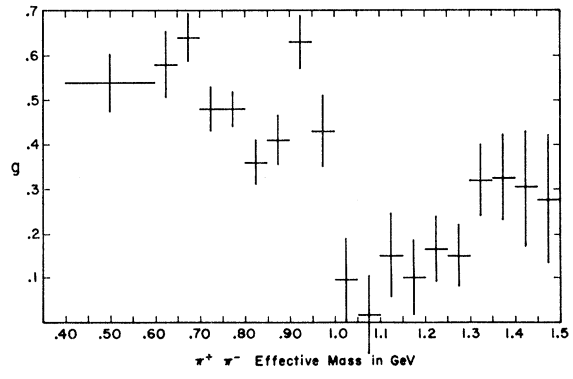

FIG. 21. Forward-backward asymmetry g as a function of $\pi^+\pi^-$ effective mass for $|t|<0.2$ (GeV/c)^2.

[6] J. D. Jackson, Rev. Mod. Phys. **37**, 484 (1965); D. H. Miller, L. Gutay, P. B. Johnson, F. J. Loeffler, R. L. McIlwain, R. J. Sprafka, and R. B. Willmann, Phys. Rev. **153**, 1423 (1967).

[7] L. J. Gutay, P. B. Johnson, F. J. Loeffler, R. L. McIlwain, D. H. Miller, R. B. Willmann, and P. L. Csonka, Phys. Rev. Letters **18**, 142 (1967).

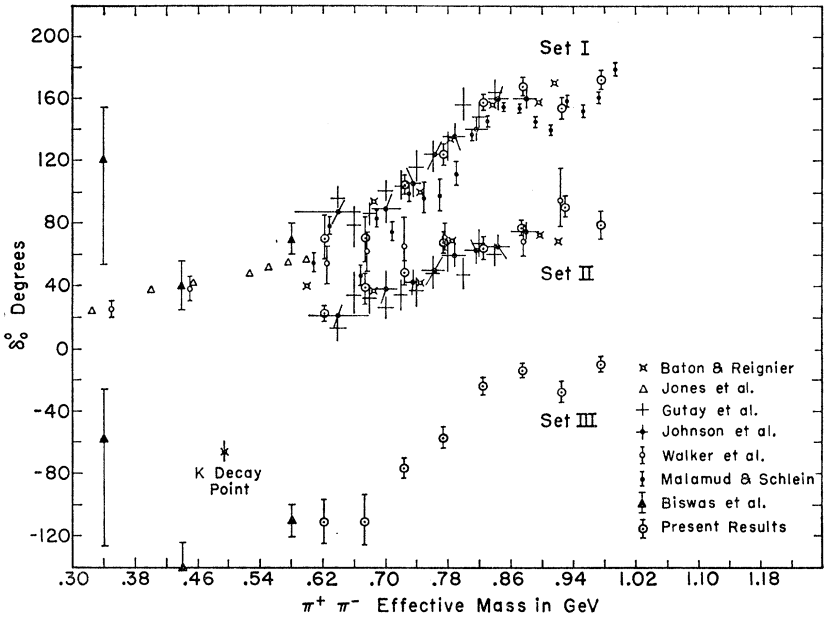

FIG. 22. The $I=0$, S-wave $\pi\pi$ phase shift as a function of the dipion effective mass. The various results are taken from the following references: J. P. Baton and J. Reignier, Nuovo Cimento **36**, 1149 (1965); L. W. Jones, D. O. Caldwell, B. Zacharov, D. Harting, E. Bleuler, W. C. Middlekoop, and B. Elsner, Phys. Letters **21**, 590 (1966); and Refs. 4, 7, 10–12 in the text.

and P-wave interference, arises from the invariance of the interference term under the transformation $\delta_0^0 \rightarrow \frac{1}{2}\pi - (\delta_0^0 - \delta_1^1)$.[7] Here δ_J^I denotes the phase shift for isospin I and angular momentum J.

In the present collaboration, we have calculated the isoscalar S-wave $\pi\pi$ phase shifts from the asymmetry parameter

$$g=(F-B)/(F+B), \tag{6}$$

where F is the number of events with $\cos\theta_{\pi\pi}>0$ and B is the number of events with $\cos\theta_{\pi\pi}<0$. When the dipion angular distribution was fitted to the form

$$U(\theta,m,t)=a(m,t)+b(m,t)\cos\theta+c(m,t)\cos^2\theta, \tag{7}$$

it was observed[4,7] that the ratio b/c was effectively independent of t and a/c was strongly dependent on t. In terms of (7), the asymmetry is

$$g=\frac{b/c}{\frac{2}{3}+2a/c}. \tag{8}$$

In Fig. 21 we show g as a function of $m_{\pi\pi}$ for $|t|<0.2$ (GeV/c)^2. We have assumed b/c to be independent of t consistent with the results of Refs. 4 and 7.

The phase shifts δ_0^0 are obtained by solving the equations

$$\tan\delta_1^1=\frac{\sin 2\delta_0^0}{3g\alpha(\delta_0^0,\delta_0^2)/\beta(\delta_0^0,\delta_0^2)-2\sin^2\delta_0^0}, \tag{9}$$

where

$$\alpha=1+k\left[\frac{4\sin^2\delta_0^0+\sin^2\delta_0^2+4\cos(\delta_0^0-\delta_0^2)\sin\delta_0^0\sin\delta_0^2}{27\sin^2\delta_1^1}\right] \tag{10}$$

and

$$\beta=1+\left[\frac{\cos(\delta_0^2-\delta_1^1)\sin\delta_0^2}{2\cos(\delta_0^0-\delta_1^1)\sin\delta_0^0}\right]. \tag{11}$$

The values of δ_1^1 used in (9) are from a relativistic calculation.[8] The values of δ_0^2 were taken from Baton *et al.*[9] The parameter k in (10) is the correction introduced by the t dependence of a/c and was varied between 1.0 and 0.25; these limits were suggested by the results cited

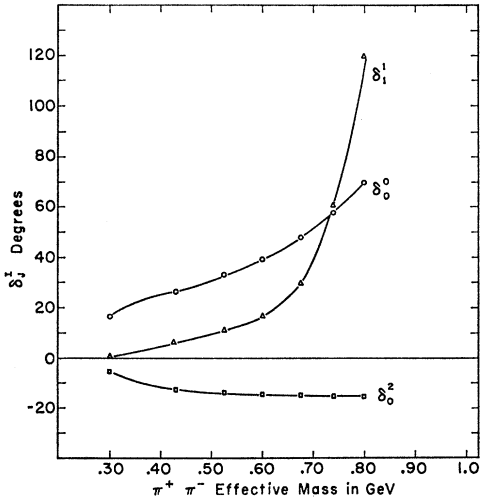

FIG. 23. The δ_0^0, δ_0^2, and δ_1^1 $\pi\pi$ phase shifts as functions of the dipion effective mass. δ_0^0 is calculated from scattering length parameters suggested by Bander (see text). δ_0^2 is taken from Ref. 9.

[8] J. S. Ball and M. Parkinson, Phys. Rev. **162**, 1509 (1967).
[9] J. P. Baton, G. Laurens, and J. Reignier, Phys. Letters **25B**, 419 (1967).

above[7] based on an absorption model. The dependence of the solution δ_0^0 on k was treated as part of the uncertainty in δ_0^0.

In Fig. 22 we show the calculated δ_0^0 as a function of $M(\pi,\pi)$ together with some results reported by other groups. The sets labeled I and II are related to each other by the interference term ambiguity. Set III is shifted by 180° from set I. The results of Walker *et al.*[10] were obtained by a method similar to that of Ref. 7 except that a constant correction factor was applied to the data to account for absorption effects. The set of δ_0^0 preferred by Walker *et al.* is seen to be in qualitative agreement with set II. Malamud and Schlein[11] fitted the dipion-decay angular distribution in the ρ helicity frame to obtain the S-wave phase shifts. We see that the set of δ_0^0 preferred by Malamud and Schlein is in good agreement with set I in Fig. 22. A recent determination of δ_0^0 at low $M(\pi,\pi)$ from interference between Coulomb and strong interaction amplitudes[12] is consistent with sets I and III.

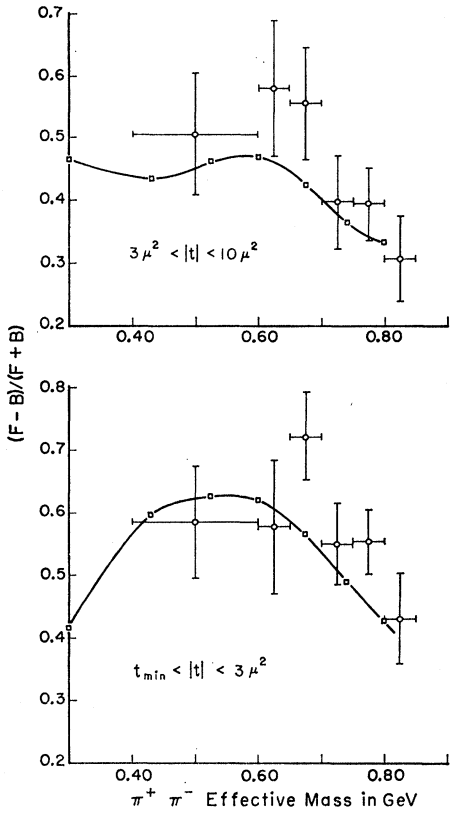

FIG. 24. The forward-backward asymmetry as a function of $\pi^+\pi^-$ effective mass for $|t|<3\mu^2$ and for $3\mu^2<|t|<10\mu^2$. The curves are calculated from the phase shifts in Fig. 23 and the model in Ref. 13.

[10] W. D. Walker, J. Carroll, A. Garfinkel, and B. Y. Oh, Phys. Rev. Letters **18**, 630 (1967).

[11] E. Malamud and P. E. Schlein, Phys. Rev. Letters **19**, 1056 (1967).

[12] N. N. Biswas, N. M. Cason, P. B. Johnson, V. P. Kenney, J. A. Poirier, W. D. Shephard, and R. Torgerson, Phys. Letters **27B**, 513 (1968).

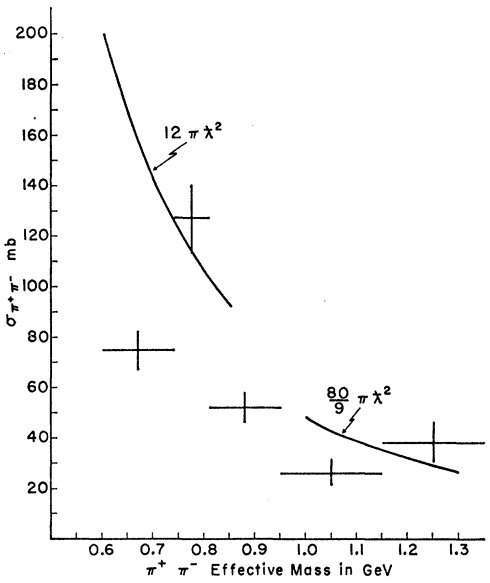

FIG. 25. The elastic $\pi^+\pi^-$ cross section obtained from an extrapolation to the pole as a function of the $\pi^+\pi^-$ effective mass. The curves are the unitary limits for spin-1 and spin-2 particles.

It is of interest to apply the Bander, Shaw, and Fulco model,[13] which includes one-pion exchange with absorption in the initial and final states to our data for reaction (1). Figure 23 shows the result of such an analysis based on scattering length, effective range, and reso-

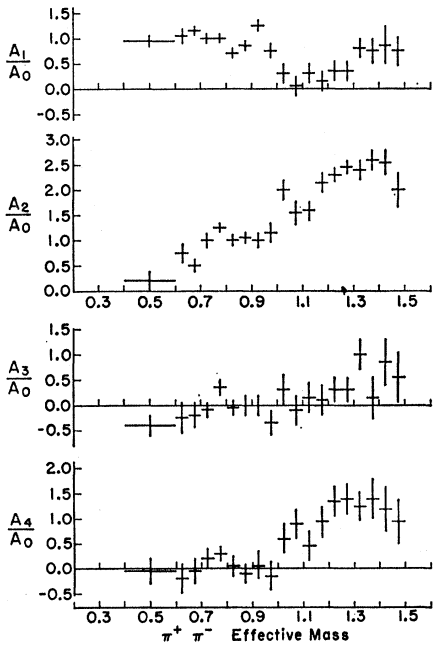

FIG. 26. Legendre coefficients from fits to the $\pi^+\pi^-$ decay angular distributions for events with $|t|<0.2(\mathrm{GeV}/c)^2$.

[13] M. Bander and G. L. Shaw, Phys. Rev. **155**, 1675 (1967); M. Bander, G. L. Shaw, and J. R. Fulco, *ibid.* **168**, 1679 (1968).

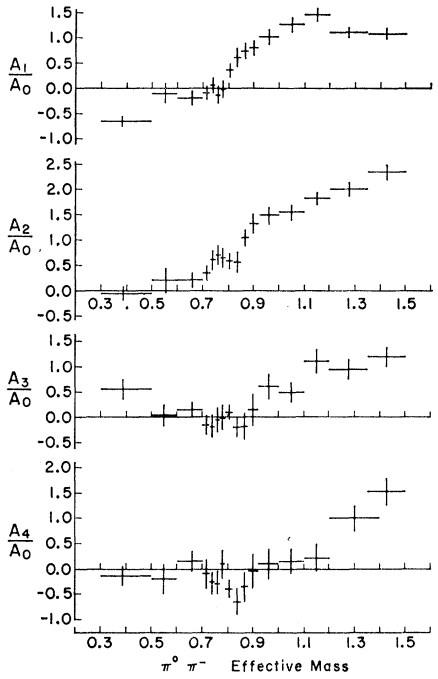

FIG. 27. Legendre coefficients from fits to the $\pi^0\pi^-$ decay angular distribution for events with $|t|<0.4(\mathrm{GeV}/c)^2$.

nance width parameters suggested by Bander.[14] The $I=2$ S-wave phase shift $\delta_0{}^2$ has been obtained from Ref. 9. It is found that this evaluation of $\pi\pi$ phase shifts is primarily sensitive to variations in the value of the ρ-meson width. The S-wave $I=0$ phase-shift $\delta_0{}^0$ solution thus obtained is found to be in qualitative agreement with that of set II of Fig. 22. In Fig. 24 we show the forward-backward $\pi\pi$ asymmetry ratio for $t_{\min}<|t|<0.06(\mathrm{GeV}/c)^2$ and for $0.06<|t|<0.2(\mathrm{GeV}/c)^2$, together with the predictions of this phase-shift analysis. The agreement is found to be adequate.

In principle, the $\pi\pi$ elastic cross section and phase shifts can be determined from a Chew-Low extrapolation.[15] Such a procedure has been used recently by Baton *et al.* to obtain the ρ^- parameters and the $I=2$ S-wave phase shift.[9] We have performed the extrapolation to obtain the $\pi^+\pi^-$ cross section; the results are presented in Fig. 25. The cross section passes through the limits $12\pi\lambda\!\!\!^{-2}$ for P-wave and $(80/9)\pi\lambda\!\!\!^{-2}$ for D-wave scattering near 0.77 and 1.25 GeV, as expected for the ρ^0 and f^0 resonances. Our statistics, however, do not permit an accurate determination of the S-wave phase shifts from such an extrapolation.

The $\pi^+\pi^-$ and $\pi^0\pi^-$ decay angular distributions have been fitted to a Legendre polynomial expansion of the form

$$1+[1/A_0(m_{\pi\pi})]\sum_{j=1}^{10}A_j(m_{\pi\pi})P_j(\cos\theta_{\pi\pi}). \quad (12)$$

The first four terms of these expansions are shown in Fig. 26 for reaction (1) and Fig. 27 for reaction (2). In almost all cases, higher-order terms were consistent with zero. For reaction (1) only events with $|t|<0.2(\mathrm{GeV}/c)^2$ were included in the fits; the cutoff for reaction (2) was $|t|<0.4(\mathrm{GeV}/c)^2$. Notice that for the $\pi^+\pi^-$ data, the A_1/A_0 term in Fig. 26 is large and positive throughout the ρ^0 region, goes through a maximum at about 0.92 GeV, and falls off to a minimum close to zero near 1.07 GeV. In the $\pi^0\pi^-$ final state, the A_1/A_0 term is small and negative from 0.5 to 0.8 GeV and increases rapidly with dipion energy above 0.8 GeV. The energy dependence of A_2/A_0 for the $\pi^+\pi^-$ final state shows a peak near 1.03 GeV. This structure ($\sim$3 standard deviations) is not seen in the $\pi^0\pi^-$ data. This structure in A_2/A_0 near 1.03 GeV is also visible in the scatter plot of $M(\pi^+\pi^-)$ versus $\cos\theta_{\pi\pi}$, as seen in Fig. 14. The peaking of A_2/A_0 together with an increasing A_1/A_0 for $m_{\pi\pi}>1.0$ GeV is consistent with constructive interference between a rapidly increasing $\delta_0{}^0$ and an increasing D-wave phase shift $\delta_2{}^0$, although we are not able to rule out the possibility that the effect is due to D or higher partial waves. This is compatible with the suggestion of a resonance[16] near 1.05 GeV, such as the S^* reported in the $K\bar{K}$ system.

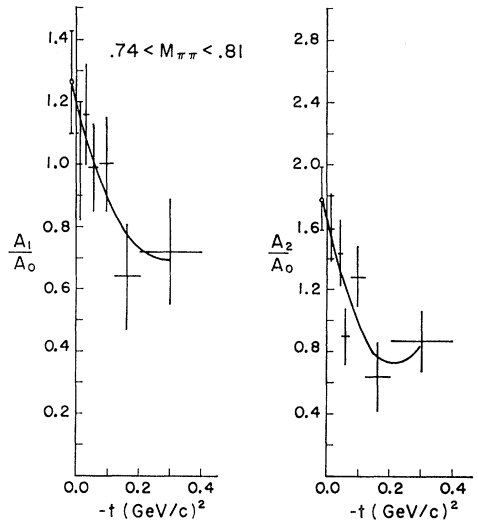

FIG. 28. The t dependence of A_1/A_0 and A_2/A_0 in the $\pi^+\pi^-$-decay angular distribution.

[14] M. Bander, University of California, Irvine (private communication to Z. G. T. Guiragossián). We would like to thank Professor Bander for several illuminating discussions, and for this computation based on our data.

[15] G. F. Chew and F. E. Low, Phys. Rev. **113**, 1640 (1959); C. Goebel, Phys. Rev. Letters **1**, 337 (1958).

[16] W. Beusch, W. E. Fischer, B. Gobbi, M. Pepin, E. Polgar, P. Astbury, G. Brautti, G. Finocchiaro, J. C. Lassalle, A. Michelini, K. M. Terwilliger, D. Websdale, and C. H. West, Phys. Letters **25B**, 357 (1967); T. F. Hoang, D. P. Eartly, J. J. Phelan, A. Roberts, C. L. Sandler, S. Bernstein, S. Margulies, D. W. McLeod, T. H. Groves, N. N. Biswas, N. M. Cason, V. P. Kenney, J. M. Marraffino, J. T. McGahan, J. A. Poirier, and W. D. Shephard, Phys. Rev. Letters **21**, 317 (1968).

A quantitative interpretation of the coefficients in Figs. 26 and 27 should be approached with some caution. Near the ρ^0 mass A_2/A_0 has a maximum value of 1.3 instead of 2.0 as expected for pure P-wave scattering.[17] This indicates the importance of absorption effects. Furthermore, in the same mass region A_2/A_0 for $\pi^0\pi^-$ is roughly a factor of 2 smaller than for $\pi^+\pi^-$. This discrepancy seems to be due to vector exchange in ρ^- production which is significant[18] near 4 GeV/c. It was pointed out above that an expansion of the angular distribution in powers of $\cos\theta_{\pi\pi}$, Eq. (7), proved particularly useful for phase-shift calculations because the ratio b/c was found to be independent of t. The terms in expression (12) are found to be strongly t-dependent. In Fig. 28 we show the results of extrapolating the Legendre coefficients A_1/A_0 and A_2/A_0 to the pion pole. The curves are least-squares fits to a quadratic form in t. Both coefficients are seen to depend strongly on t and the values at the pole have large errors associated with them.

We suggest that it is highly desirable to extend S-wave $\pi\pi$ phase-shift calculations to dipion masses greater than 900 MeV. A phase-shift analysis offers the best means of settling questions about possible resonances between the ρ^0 and f^0. Also, it would help determine which of sets I and II is the correct set for $\delta_0{}^0$ since set I approaches 180° and set II is near 90° at 900 MeV.

[17] For P-wave and S-wave amplitudes

$$A_2/A_0=6\sin^2\delta_1{}^1/[(4/9)\sin^2\delta_0{}^0+3\sin^2\delta_1{}^1].$$

If $\delta_0{}^0=\frac{1}{2}\pi$ when $\delta_1{}^1=\frac{1}{2}\pi$, then $A_2/A_0=1.74$.

[18] W. L. Yen, R. L. Eisner, L. Gutay, P. B. Johnson, P. R. Klein, R. E. Peters, R. J. Sahni, and G. W. Tautfest, Phys. Rev. Letters **18**, 1091 (1967); I. Derado, J. A. Poirier, N. N. Biswas, N. M. Cason, V. P. Kenney, and W. D. Shephard, Phys. Letters **24B**, 112 (1967).

PHYSICAL REVIEW VOLUME 176, NUMBER 5 25 DECEMBER 1968

Experimental Tests of Cascade Theory at High Energies*

R. HOLYNSKI† AND W. V. JONES‡
Department of Physics and Astronomy, Louisiana State University, Baton Rouge, Louisiana 70803

AND

K. PINKAU
Max-Planck-Institut für Extraterrestrische Physik, Garching bei München, Germany

(Received 1 July 1968)

Results of simultaneous measurement of the radial position and angular orientation of electrons in ten high-energy (180–2000-BeV) electromagnetic cascades are given. Six of these cascades were developed in pure emulsion, while four were developed in a lead-emulsion sandwich stack. Numerical calculations of the angular distributions, both within approximation B and the core approximation, are presented. Calculations on the mixed radial-angular distribution are related to the separate distributions. A method is given for the use of the mixed distribution to extend the effective radial range of measurement to such an extent that the transition of the experimental results from the core approximation to approximation B becomes evident. Limited experimental verification of the often-used approximation B is thereby established. It is further shown that cascade theory is internally consistent within the region of validity of the core approximation and that the radial range must extend up to $\sim 10^{-1}$ radiation length in order to include all particles having angles as small as ~4–5 deg.

I. INTRODUCTION

THE measurement of the lateral distribution of cascade electrons offers one of the few possibilities to measure the energy of ultrahigh-energy particles ($\geq 10^{11}$ eV). Such measurements rely on the experimental determination of the radial distribution of the cascade electrons at specified distances from the cascade origin.[1] The experimental results are then compared with the theoretical calculation of the integral radial distribution in the three-dimensional cascade theory.[2] These theoretical calculations utilize an approximation which requires that the radius R be small compared to unity when expressed in units of the radiation length (r.l.). This is called the "core approximation"[3] since it is valid only near the core of a cascade.

Experimental evidence, which has been obtained from scattering measurements on individual cascade

* Work supported by the National Science Foundation.

† On leave of absence from Institute of Nuclear Research in Krakow, Poland.

‡ Submitted in partial fulfillment of the Ph.D. degree at Louisiana State University, Baton Rouge, La. W. V. J. would like to express his appreciation for an NDEA Graduate Fellowship at Louisiana State University, and he would also like to thank the Alexander von Humboldt Stiftung in Germany for a research stipend at the Max-Planck-Institut für Extraterrestrische Physik, Garching bei München, Germany.

[1] K. Pinkau, Phil. Mag. **2**, 1389 (1957).

[2] K. Kamata and J. Nishimura, Progr. Theoret. Phys. (Kyoto) Suppl. **6**, 93 (1958).

[3] K. Pinkau, Nuovo Cimento **33**, 221 (1964).